

Effect of the Performance of Lignin Into the Matrix of the TiO₂ with Application on DSSCs

Edwalder Silva Teixeira¹ 

Vanja Fontenele Nunes¹

Diego Caitano Pinho¹

Paulo Herbet França Maia Júnior¹

Francisco Marcone Lima¹

Men de Sá Moreira de Souza Filho²

Ana Fabíola Leite Almeida¹

Francisco Nivaldo Aguiar Freire¹

¹Universidade Federal do Ceará (UFC), Fortaleza, CE, Brasil.

²Embrapa Agroindústria Tropical, Fortaleza, CE, Brasil.

Abstract

Founding new materials and structures for solar cells is a challenge in the photovoltaic field. This work evaluated the effect of the lignin in the photovoltaic activity by compounding with TiO₂/lignin as photoanode for the dye sensitized solar cells (DSSC's). Hybrid films (TiO₂/lignin) with different concentrations of lignin (5, 10 and 15%) were deposited by spin coating over commercial TiO₂ thin films. The cells were sandwich assembled. The characterizations were done through analysis of absorbance, band gap, x-ray diffraction, morphological and electrical. The lignin at 15% reduced the TiO₂ band gap from 3.66 to 2.84 eV, favoring the short current density to 11.06 mA/cm² and efficiency of 4.65%, an increase of 103.95% compared to the TiO₂ structure without lignin.

Keywords: Lignin, TiO₂, DSSCs, Spin coating.

1. INTRODUCTION AND OBJECTIVES

The dye sensitized solar cells (DSSCs) since developed by Michael Grätzel and O'Regan in 1990, are promising alternatives for photovoltaic devices, due to low fabrication costs and easy assemble (Al-Attafi et al., 2017; Fan K et al., 2017; Grätzel M, 2003; Kakiage K et al., 2015; O'Regan B & Grätzel M, 1991).

In the DSSCs, the TiO₂ (titanium dioxide) is one of the most used photoanodes due to the lower costs, when faced with silicon used on the first generation solar cells, high photocatalytic activity, chemical resistance to different conditions, excellent conduction on the conduction band, low toxicity and abundance (Donar YO et al., 2020; Bezira NÇ et al., 2017).

The TiO₂ has two structures, anatase (band gap energy (Eg) = 3.2 eV) and rutile (Eg = 3.0 eV). Both structures of the pure TiO₂ absorb energy only on the ultraviolet area of the solar spectrum, which can be a disadvantage, since 40% of the solar energy incident on the earth surface lies on the

visible range. Therefore, for the TiO₂ to be used on the DSSC is necessary to apply supportive materials to absorb light in this visible range (Müller AV et al., 2021).

Many strategies can be used to improve the TiO₂ photoanode absorption in the visible range of the solar spectrum, besides to reduce the effects of the recombination between the pair electron-hole and increase the DSSC's efficiency. As example, the doping with metallic and non-metallic materials in the TiO₂ structure, like Al (aluminum)/N(Nitrogen) (Dhonde KS et al., 2018), Cu (Copper)/N (Dhonde M et al., 2021) Cu/S (sulfur) (Gupta A et al., 2020) and carbon nonmetallic materials, graphene (Dhonde M, 2018) and carbon nanotubes (Lee CH et al., 2012). All of these incorporated in the TiO₂ matrix presented high porosity area, high specific superficial area and more dye adsorbed in the TiO₂ surface, which favors the short current density (Jsc), upping the efficiency of the DSSCs (η = 11.08% (Dhonde KS et al., 2018), η = 11.70% (Dhonde M, 2018), η = 10.44% (Gupta A et al., 2020), η = 9.81% (Dhonde M et al., 2021), η = 4.57% (Lee CH et al., 2012)).

By taking the components and the devices to be used on the energy conversion and storage, the organic nature of the materials in the DSSCs photo electrodes has been considered. Nano cellulose fibers extracted from lilies incorporated in the TiO₂ matrix, resulted in a highly porous structure, with higher dye adsorption and luminous energy conversion efficiency into electricity, $\eta = 2.30\%$ (Saleem et al., 2021). In other work, the fibers were extracted from the taboa plant to be added in the TiO₂ matrix, to increase the superficial area and the results indicated $\eta = 2.95\%$ (Abbas Q et al., 2020).

Lignin (LG) is a tridimensional aromatic molecule with amorphous structure, considered the second most abundant natural vegetal polymer, after cellulose (Leonowicz et al., 1999; Lu Y et al., 2017). It is responsible for mechanical resistance, vegetable elasticity, and tissue protection against microorganisms, besides a high concentration of carbon (García-Negron V et al., 2017). Lignin has been used to produce carbon nanotubes (Gindl – Altmutter W et al., 2019), as an organic alternative to the fossil materials.

Although having a complex structure, LG has called the attention of the scientific community due to its low cost, natural abundance and renewability (Klapiszewski Ł et al., 2017). The reason for the use of the lignin in the DSSCs is associated with the capacity to increase the adsorption area for the electrolytic solution on the semiconductors porous, wit, also, higher dye area adsorption, and, consequently, the solar cell efficiency (Khan A et al., 2018).

In the present work, it is described the effect of the lignin on the TiO₂ matrix, to improve the efficiency of the DSSCs and also to investigate the morphological and optical alterations of the lignin on the TiO₂.

2. MATERIALS AND METHODS

The lignin kraft was acquired from the company Suzano and the TiO₂ (Aldrich) (99%), anatase phase and the average particle size 21 nm was used to compose a hybrid semiconductor with lignin. The commercial glass with TiO₂ opaque was from Solaronix (74101) with an active area of 0.25 cm² and dimensions of 25 x 25 x 2 mm and it was used to deposit the hybrid TiO₂/lignin film, multilayer film. All the products (Aldrich, Vetec, Dynamic, Suzano and Solaronix) were used without any additional purification.

2.1. Preparation and deposition of the solution TiO₂/Lignin

The commercial glass (Solaronix – 74101) of the TiO₂ opaque deposited by glass rod were used for the deposition

by spin coating of the hybrid TiO₂/lignin in the following proportion: 95/5(wt%) (EST5LG), 90/10(wt%) (EST10LG) and 85/15(wt%) (EST15LG).

The solution was prepared by adding 1.5 g of TiO₂ in isopropyl alcohol (1 mL) and agitated for 15 minutes in a magnetic stirrer. The amount of lignin used in proportion to the TiO₂, 95/5(wt%), 90/10(wt%) and 85/15(wt%), and the TiO₂ were added to the isopropyl alcohol (1 mL) and agitated for 15 minutes by magnetic stirrer. Following, the lignin mass in proportion to the TiO₂ was solubilized in solution of: 1:1 (Dimethyl Sulfoxide - (DMSO)/ isopropyl alcohol), with 0.25% (m/m) Triton X and 20% (m/m) glycerol and taken to ultrasound bath for 15 minutes.

The solution TiO₂/lignin, 0.08 mL, was deposited on TiO₂ opaque commercial (Solaronix – 74101) at rest. Next, it was rotated at 1800 (rpm) for 15 seconds and, in the end, at 5000 (rpm) for 15 seconds for the evaporation of the solvents still present, to control the thickness and the homogeneity of the film. After the deposition, the glass was heated in a muffle furnace at 450°C for 30 minutes at a rate of 10°C/minutes.

2.2. Assemble of the dye sensitized solar cell (DSSCs)

The thin films of TiO₂/lignin were deposited by spin coating on the commercial TiO₂ opaque (Solaronix) to compose the hybrid semiconductors. All the photoanodes (PAs) formed with the TiO₂ semiconductor with and without lignin had an active area of 0.25 cm².

The PAs ((EST5LG, EST10LG and EST15LG) were immersed in a solution of isopropyl alcohol and N719 dye (Solaronix) (0.0003 M) for a period of 24 hours. Following, the cells were sandwich assembled with a counter electrode (CE) of platinum (Pt) (Solaronix). The sandwich assembled structures were linked through a thermoplastic polymer (Surlyn@ 1702) and heated at 60°C for 1 minute. Between the PAs and CE an electrolytic solution with the pair iodide/triiodide NA-50 (Solaronix) was injected. The same methodology can be found at (Grätzel M, 2003; Graetzel M et al., 2012; Jeng MJ et al., 2013; Mathew S, 2014; Ito S et al., 2006).

3. RESULTS AND DISCUSSION

3.1. Optical characterization

The spectrum of optical absorption of the thin films TiO₂ and TiO₂/Lignin deposited by spin coating were done at room temperature in a Cary100 UV-Vis (UV-VIS), with wavelength between 220-800 nm.

Figure 1 illustrates the spectrum of optical absorbance of the films of TiO_2 and $\text{TiO}_2/\text{lignin}$ (EST5LG – 5%, EST10LG – 10%, EST15LG – 15%) after dyeing for 24 h with the N719. The range where there is the luminous energy into electricity conversion corresponds to the 400–700 nm intervals, on the visible range of the solar spectrum (Wang X et al., 2021). And, facing the results indicated in the spectrum of the 15% lignin sample (EST15LG) in the TiO_2 matrix, this sample was the one with higher optical absorption in the visible range, with a peak at 522 nm. This peak in the visible range (522 nm) fits the required to an efficient photons collector to the conversion of luminous energy into electricity in the DSSCs (Ghann W et al., 2017). This higher absorption may have happened due to the thicker structure of the films and higher dye adsorption on the $\text{TiO}_2/\text{lignin}$ thin surface, with a possible lower band gap. And, the introduction of the dopant elements in the TiO_2 structure is one of the strategies to modify the photoanodes to increase the photons capture to favor better efficiency of luminous energy into electricity conversion in DSSCs (O'Regan B and Grätzel M, 1991; Wang X et al., 2021; Matthews D et al., 1996; Kumari JMKW et al., 2016).

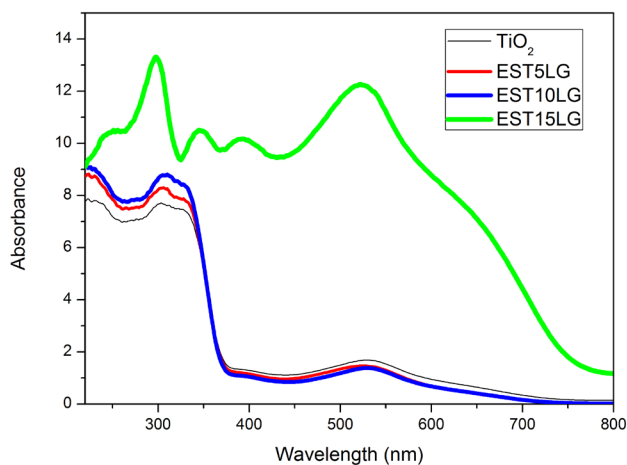


Figure 1. Spectrum of optical absorbance of the films (EST0LG, EST5LG, EST10LG and EST15LG) versus wavelength after dye (24 h).

After the optical analyses of the films (Figure 1), it is possible to infer that the 15% lignin film (EST15LG) in the TiO_2 matrix had the better performance in the optical characterization. The optical results are related not only to the amount of lignin but, also, with the band gap, morphology, thickness and other parameters. It is important to notice that the higher thickness of the film increases the absorption on the spectrum (Matthews D et al., 1996; Kumari JMKW et al., 2016; Nunes VF et al., 2021). This directly affects the solar cell efficiency, because the photons that are captured

by the dye molecules perform the chemical adsorption in the TiO_2 surface, making more absorbed photons to achieve photoelectric conversion (Kumari JMKW et al., 2016) and better performance of the DSSCs (Matthews D et al., 1996; Kumari JMKW et al., 2016).

3.2. Band gap energy

Band gap energy (E_g) was estimated using Kubelka-Munk, with the values $(F(R) \cdot hv)^n$ versus (hv) , where for the indirect transition $n=2$ (Aba-Guevara et al., 2017). The E_g is estimated assuming that the Kubelka-Munk function $F(R)$ is close to zero (Figure 2). The results of the band gap (Figure 2) for the films with 5% (EST5LG), 10% (EST10LG) and 15% (EST15LG) of lignin in the TiO_2 matrix were, respectively, 3.66 eV, 3.43 eV and 2.84 eV. With these results, it is possible to understand that the films with 15% lignin (EST15LG) in the TiO_2 matrix (Figure 2), had the lowest band gap energy, 2.84 eV, lower than the values of the TiO_2 anatase phase (3.2 eV) (Etacheri V et al., 2015; Jeng MJ et al., 2013; Guo D et al., 2020). Low band gap energy values implicate lower resistance and more flux of electrons from the valence band, with added energy, to the conduction band of the semiconductor and higher solar cell efficiency (Wang X et al., 2021; Etacheri V et al., 2015).

The pure TiO_2 (band gap 3.2 eV) does not absorb light in the visible range of the solar spectrum (Ghann W et al., 2017) and the lower band gap favor a better DSSCs performance (Garcia – Negrón V et al., 2017; Wang X et al., 2021; Matthews D et al., 1996; Kumari JMKW et al., 2016). Once the introduction of the lignin in the matrix of the TiO_2 lowered the band gap values below 3.2 eV, there was higher absorption of light in the visible range of the solar spectrum.

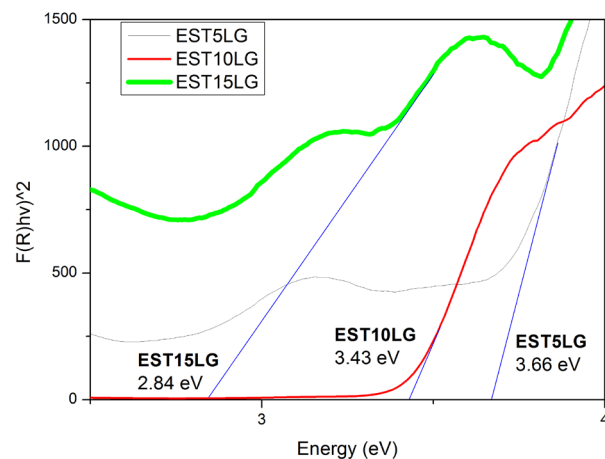


Figure 2. Band gap energy of the films EST5LG, EST10LG and EST15LG.

3.3. SEM (Scanning Electron Microscopy) and EDS (Energy Dispersive Spectroscopy)

The morphological characterizations of the films EST5LG, EST10LG, EST15LG and the quantitative analyses of the elements in the TiO₂/lignin films were done using a SEM microscope Quanta 450 FEG-FEI (Figures 3a, b and c), with a EDS detector connected (Figures 4a, b and c).

It was observed particles spherically shaped and the presence of agglomerated with the higher proportion of the lignin in the TiO₂ matrix (Figures 5a, b and c). This geometry is expected for the TiO₂ particles (Jeng MJ et al., 2013; Guo D et al., 2020; Pan K et al., 2011; Barbé CJ et al., 1997; Ni M et al., 2006). To obtain the information about the average diameter and the porous distribution, the software ImageJ, broadly used in research, was applied (Figure 5a, b and c, Table 1) (Chilev C et al. 2017).

The introduction of the lignin in the matrix of TiO₂ increased the surface area (0.490 nm²) and the average porous diameter (178.6 nm) of the film with higher lignin proportion (15% of lignin – EST15LG) in the TiO₂ matrix (Figure 5c, Table 1). The increase in the surface area and the particle's average diameter is important to improve the quantitative adsorption of dye in the TiO₂ surface, more photons can be adsorbed in the semiconductor surface, affecting the electrolytic migration and the solar cell efficiency (Huang WY and Hsieh TL, 2019).

Table 1. Average porous diameter and films thickness.

Description	Superficial area (nm ²)	Average porous diameter (nm)	Thickness (µm)
EST5LG	0.322	116.5	1.66
EST10LG	0.371	134.6	1.84
EST15LG	0.490	178.6	2.59

The average porous size also impacts the film's thickness and consequently the efficiency of the solar cells (Jeng MJ et al., 2013). The film's thickness measurements were obtained through SEM images of the transversal section of the films (Figuras 3a, b and c). In Table 1. It is seen that the film with higher porous diameter (178.6 nm) was the thicker out of all (2.59 µm) (Figure 5c). The ideal thickness depends on the size of the particles for the maximum solar cell efficiency. However, the ideal thickness is not the same for all cells. For example,

(Baglio V et al., 2011) analyzed the behavior of the thin films of TiO₂ with different thickness (6, 10 and 14 µm) fabricated through spray pyrolysis in DSSCs. The cell assembled with the TiO₂ at 10 µm that had better performance $\eta = 1.44\%$. (Kumari, JMKW et.al., 2016) analyzed the thickness of the titanium dioxide by doctor blade in the parameters of the photoanodes in the DSSCs. The films had thickness between 5.57 µm and 20.65 µm. The results indicated that the film with 12.73 µm had better performance of $\eta = 6.07\%$. In other work, (Teixeira ES et al., 2020) deposited thin films of TiO₂ by spin coating with different thickness (65.90, 90.17, 106.7 µm). The results indicated that the cell assembled with TiO₂ of thickness 65.90 µm presented $\eta = 12.74\%$. It is important to mention that from 20% of lignin in the matrix of TiO₂, thickness (4.55 µm), the solar cell started to decline in its efficiency. As such, the ideal thickness for the hybrid TiO₂/lignin was 2.59 µm with 15% of lignin. Adding, the higher thickness hinders the photoexcitation of the electrons from the adsorbed dye into the layer, which blocks the formation of excitons (electron-hole) pairs in the interface.

And the analyses of the EDS (Figure 4a, b and c) of the hybrid films TiO₂/lignin allowed identifying the two peaks present in the samples, that were the titanium (Ti) and the oxygen (O), which are the main elements of the TiO₂. By studying the relative proportions of the quantities (Wt%) of the main elements (Ti/O) in a specific area, the proportions were as follows: 4.54 (film EST5LG), 4.10 (film EST10LG) and 3.5 (film EST15LG). Such reduction allows a higher superficial area and consequently higher grain size and more dye can be absorbed into the film surface for more efficiency of the photocurrent of the solar cell (Mahmoud AS et al., 2021).

The presence of Na (sodium) on the samples of FTO and the S (sulfur) due to the process of extraction of the kraft lignin, which uses the sodium sulfite (Na₂S) to isolate the lignin in the cellulose and the hemicellulose (Khan A et al., 2018; Ibrahim MNM et al., 2019) and the presence of P (phosphorous) in all samples happened due to the interactions of the lignin with the TiO₂ matrix, which eases the conversion of luminous energy into electrical.

It is seen that the introduction of lignin in the TiO₂ matrix makes films with particles of diameters size bigger and consequently higher adsorption dye area and more photons captured to favor the current density in the process of conversion of luminous energy into electricity

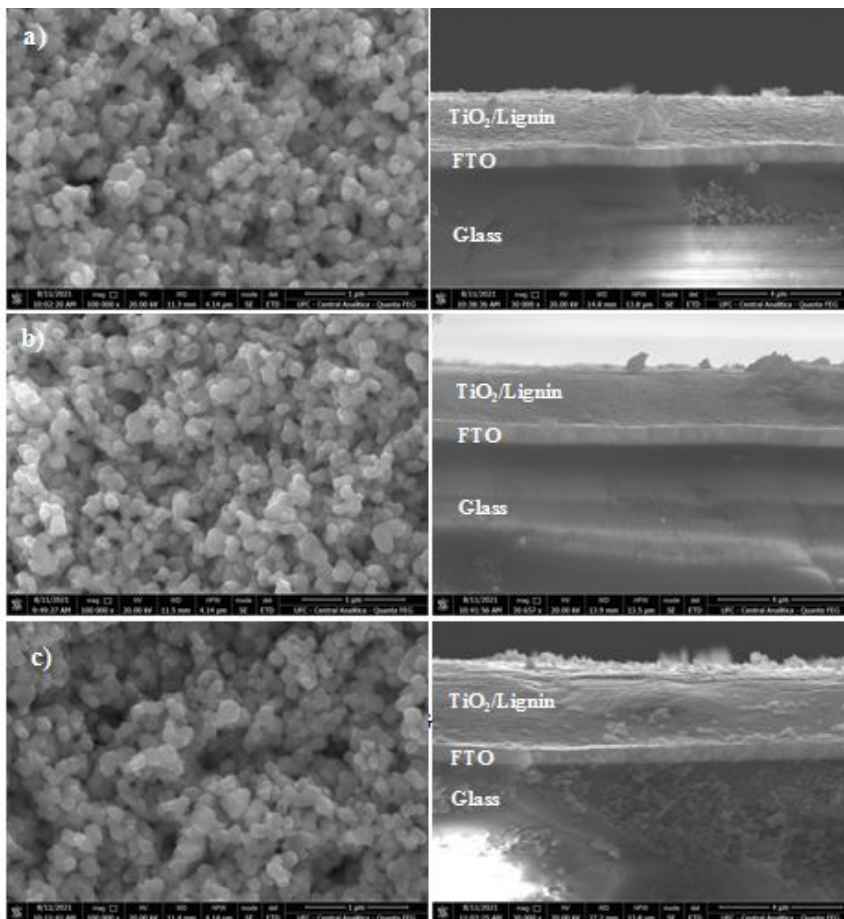


Figure 3. SEM analysis of the distribution of agglomerates and the films thickness EST5LG (a), EST10LG (b) and EST15LG (c).

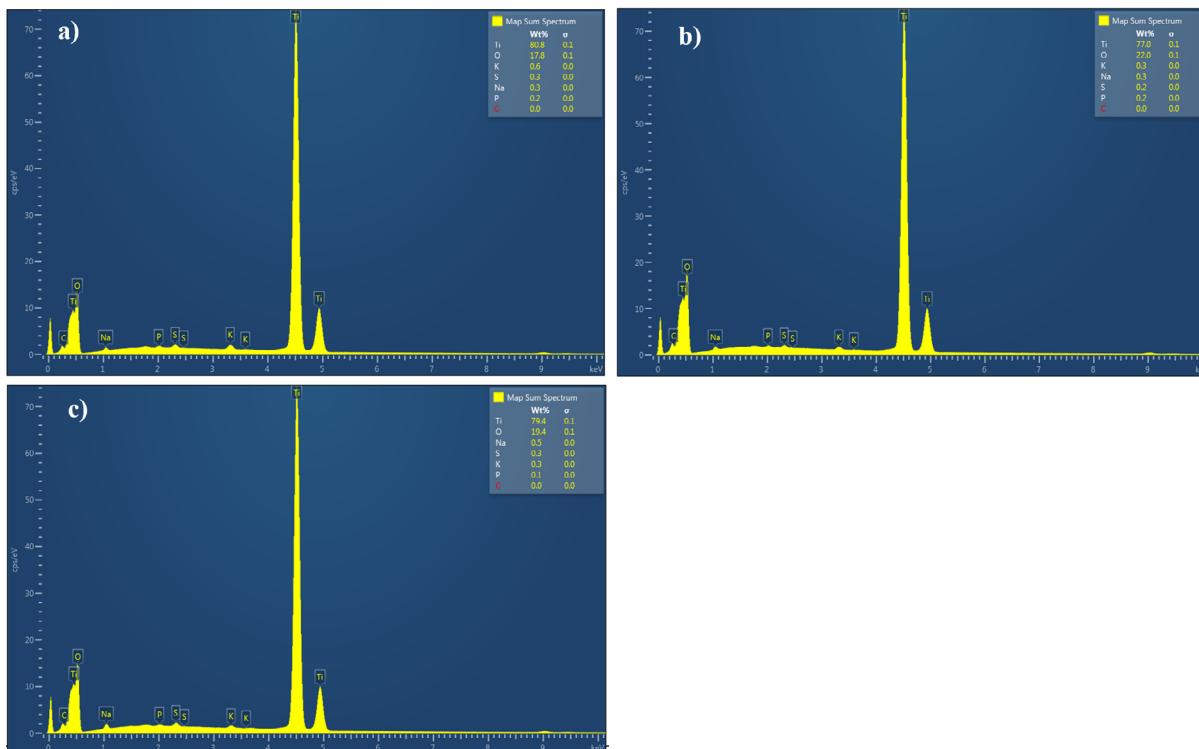


Figure 4. Film EDS data (EST5LG (a), EST10LG (b) and EST15LG (c)).

3.4. X-Ray

With the results of the optical, SEM and band gap characterizations, the sample EST15LG was chosen to identify the phases present and the characterizations through diffractometer and x-ray with a x-ray diffractometer (Rigaku DMAXB), with geometry Bragg-Brentano in continuous mode with speed 0.25 °/min. The source of radiation used was the Cu-K α of $\lambda = 0.154$ nm, with linear focus operating at 40 kV and 25 mA. The diffraction patterns were obtained between $2\theta = 10$ -90°.

The spectrogram of the film EST15LG (Figure 5) is represented through the peaks of the indexed elements (101), (103), (200), (105), (211), (204), which indicated the scattering angles respectively 25.32, 36.98, 48.06, 53.94, 55.08 and 62.7 degrees. This pattern of diffraction is similar to the TiO₂ commercial anatase phase, ICSD collection code 009852, which is indicated through the scattering angles: 25.308, 36.951, 48.047, 53.885, 55.073 and 62.692 degree (Donar YO et al., 2020). The peaks 26.47 and 51.47 degrees indicated the structure of an amorphous material, confirming that the lignin is a material of amorphous nature (Donar YO et al., 2020; Guo D et al., 2020). With the spectrum, it was confirmed that the sample EST15LG was indeed TiO₂ anatase phase and that the introduction of lignin in the TiO₂ did not alter significantly its structure.

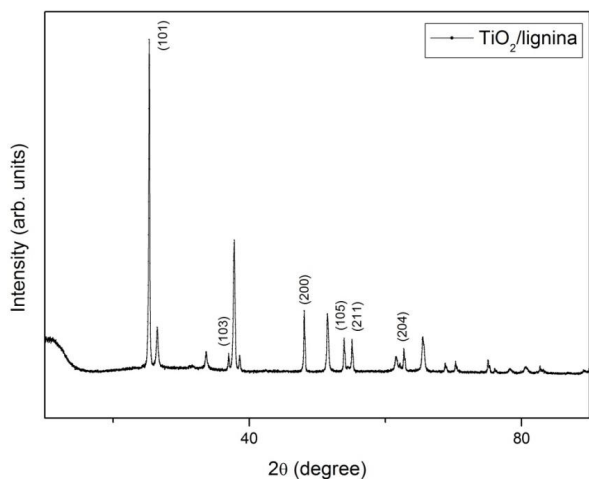


Figure 5. X-Ray of the film TiO₂/lignin (EST15LG).

3.5. Electrical characterization of the solar cells (DSSCs)

The DSSCs were electrically characterized using the potentiostat/galvanostat PGSTAT302N (Metrohm, Switzerland) to obtain the curves of current density (Jsc) versus voltage (V) and the measures of incident photos conversion to electrical

current efficiency (IPCE). The J-V measurements and the IPCE were obtained under simulated solar illumination LED with 100 mW/cm².

The characterization of the J-V measurements is a method to determine the capacity of the DSSCs to convert solar light into electrical energy (O'Regan B and Grätzel M, 1991; Grätzel M, 2003; Michael Graetzel et al., 2012).

J-V measurement is a tool well known to evaluate the different types of photovoltaic solar cells. The J-V measurement describes the behavior of the solar cell and was adopted in this work because it is broadly used in the characterization of commercial solar cells.

From a specified tension, the product of the energy density (I x V) at maximum value (J x V)max drops abruptly until zero, where I is the current (Souza APS et al., 2020). From the characteristics J-V (Figure 6) was possible to obtain the short circuit current (Jsc), the open circuit voltage (Voc) and the fill factor (FF), and, with this data it was found the efficiency of the solar cell, equation 1 (O'Regan B and Grätzel M, 1991).

The IPCE is a measure of how much the cell efficiency can convert monochromatic light into electrical current and it is related to the capacity of the dye to absorb incident photons (Shahrul AM at al., 2022). Overall, the IPCE can be defined with the number of electrons generated by light to an electrical circuit divided by the number of incident photons and calculated through equation 2, where λ (nm) represents the wavelength of incident wave (Shahrul AM at al., 2022).

The results of the characteristic curve J-V (Figure 6) can be visualized in Table 2. The cells were assembled with double layer films. First one was composed with the TiO₂ opaque commercial (Solaronix - 74101- 9 μ m) and the second with the TiO₂/lignin film deposited over the first by spin coating with the variation of the proportion of lignin in the TiO₂ structure. The EST5LG represents the sample with 5%, EST10LG 10% and EST15LG 15% of lignin in the TiO₂ structure, respectively.

$$\eta = \frac{V_{OC} \times I_{SC} \times FF}{P_{inc}} \quad (1)$$

$$IPCE = \frac{1239 \times J_{SC}}{\lambda(nm) \times P_{inc}} \quad (2)$$

The results of the electrical parameters of the DSSCs with different thickness of the films are indicated in Figure 6, Table 2. The current density increased from 7.55 to 11.06 mA/cm² and the total thickness from 10.66 ((9+1.66) para 11.59 μ m (9+2.59). The increase of the short current density (Jsc) which is observed for the cell (EST15LG) is associated

with the increase of the current due to the higher quantity of excited electrons from the valence band of the dye to the conduction band of the TiO_2 /lignin. This is due to the higher dye adsorption area in the TiO_2 surface, with more captured electrons, to ease the process of transfer of electron-holes from the dye to the semiconductor. According to Hagfeldt A et al., (2010), once the incident photon has been adsorbed by the dye and generated pairs of electron-holes, these charges must be separated and collected in the interface dye/semiconductor efficiently. A “good” material avoids charge recombination and, therefore, a drop in the device IPCE (Souza APS et al., 2020). With the data in Table 2, it is noticed that the IPCE arises with the increase of the thickness of films.

Additionally, for the sample with 20% of lignin in the TiO_2 matrix, there was decrease in the IPCE that indicates that a denser layer hinders the incident light dispersion reduces the photoexcitation of the adsorbed dye and contributes to a lower generated photocurrent (Souza APS et al., 2020).

Overall, to maximize the DSSCs efficiency, there is an optimum value of thickness. However, this value is not the

same for all cells; for example, TiO_2 thin films were fabricated by spin coating with an optimum thickness value of 12 μm and DSSC efficiency of 2.85% (Jeng MJ et al., 2013). The thicker layer of the film promotes dye immobilization, but can lower the conversion efficiency of the DSSCs.

The ideal thickness for the hybrid semiconductor TiO_2 /lignin was 2.59 μm with 15% lignin (EST15LG). Then, the film TiO_2 /lignin (EST15LG) with 15% of lignin in the TiO_2 matrix deposited by spin coating over the commercial opaque TiO_2 (74101) presented thickness of 11.59 μm , $J_{sc} = 11.06 \text{ mA/cm}^2$, IPCE = 21.9% and efficiency of $\eta = 4.65\%$, results 103.95% higher compared to the TiO_2 without lignin (Table 2).

Evidently that the increase on the percentage of lignin in the TiO_2 film EST15LG, increased the superficial area of the film (Table 1) and that also increased the current density, consequently higher DSSCs efficiency (4.65%), with the maximum absorption in the visible range of the solar spectrum (Kumari JMKW et al., 2016; Nunes VF et al., 2021; Aba – Guevara et al., 2017 e Etacheria V et al., 2015).

Table 2. Electrical parameters of the cells assembled with the double layer of TiO_2 commercial (Solaronix-74101)/ TiO_2 -Lignin.

First layer	Thickness (μm)	Second layer	Thickness (μm)	J_{sc} (mA/cm^2)	V_{oc} (V)	FF	IPCE	η (%)
TiO_2 Solaronix (74101)	9	EST5LG	1.66	7.55	0.7592	0.3975	14.9%	2.28
		EST10LG	1.84	8.31	0.8007	0.3987	16.4%	2.65
		EST15LG	2.59	11.06	0.7568	0.5550	21.9%	4.65
		EST20LG	4.55	7.16	0.7764	0.5868	14.15%	3.26

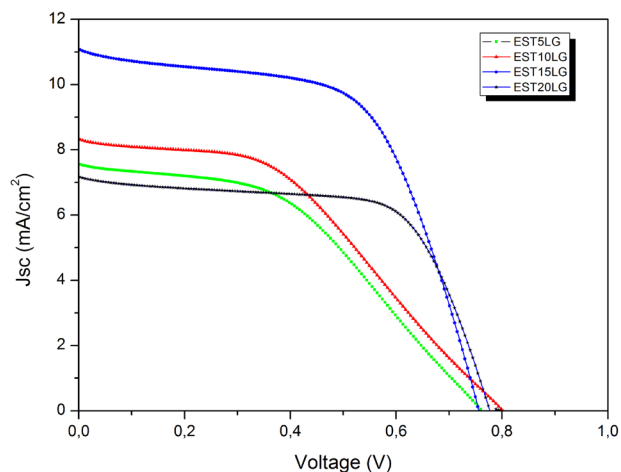


Figure 6. Films electrical data of the curves J_{sc} versus voltage (V) (EST5LG, EST10LG and EST15LG).

It is important to mention that from the 20% lignin in the TiO_2 matrix, thickness of 4.55 μm , the cell presented reduction in the IPCE (14.15%) and in the efficiency ($\eta = 3.26\%$) (Table 2).

The increase in the efficiency is caused by the organic macromolecule nature of the lignin, with OH groups that, when in contact with metallic ions, positive charge (TiO_2) creates strong interaction (Colmenares JC et al., 2016). For example, lignin with phenolic hydroxyl, alcohol hydroxyl and carboxyl groups can react chemically with other polymers to form hybrid composites (Colmenares JC et al., 2016).

Therefore, the lignin represents a strong potential to be applied with photoanodes on the DSSCs, seeing the strong interactions with TiO_2 to increase the optical light absorption in visible range of the spectrum, with higher dye adsorption area in the surface of the TiO_2 /lignin films, causing more photons to be captured and favor the efficiency of luminous energy into electricity.

4. CONCLUSIONS

The introduction of the lignin in the TiO₂ matrix in the proportions 5, 10 and 15% deposited by spin coating with application as photoanodes in the DSSCs was successful. The lignin caused optical, morphological and electrical changes. The best photovoltaic device was the one with 15% lignin in the TiO₂ matrix. The presence of 15% lignin helped to improve the photovoltaic parameters of the DSSCs, specifically the current density, 11.06 mA/cm², which was responsible for the efficiency improvement to 4.65%.

SUBMISSION STATUS

Received: 22 Feb. 2022

Accepted: 08 Jun. 2022

Associate editor: Fernando Gomes 

CORRESPONDENCE TO

Edwalder Silva Teixeira

Av. Humberto Montes, s/n, bloco 715, CEP 60440-593, Fortaleza, CE, Brasil

e-mail: edwalderteixeira@hotmail.com

AUTHORS' CONTRIBUTIONS

Edwalder Silva Teixeira: Conceptualization (Equal), Data curation (Equal), Formal analysis (Equal), Funding acquisition (Equal), Investigation (Equal), Methodology (Equal), Project administration (Equal), Resources (Equal), Supervision (Equal), Validation (Equal), Visualization (Equal), Writing – original draft (Equal), Writing – review & editing (Equal).

Vanja Fontenele Nunes: Resources (Equal), Software (Equal), Validation (Equal), Visualization (Equal).

Diego Caitano Pinho: Conceptualization (Equal), Formal analysis (Equal), Investigation (Equal), Methodology (Equal), Resources (Equal).

Paulo Herbet França Maia Júnior: Conceptualization (Equal), Data curation (Equal), Formal analysis (Equal), Funding acquisition (Equal), Investigation (Equal), Methodology (Equal), Project administration (Equal), Resources (Equal), Software (Equal).

Francisco Marcone Lima: Conceptualization (Equal), Data curation (Equal), Investigation (Equal).

Men de Sá Moreira de Souza Filho: Conceptualization (Equal), Data curation (Equal), Resources (Equal), Visualization (Equal).

Ana Fabíola Leite Almeida: Methodology (Equal), Supervision (Equal), Visualization (Equal).

Francisco Nivaldo Aguiar Freire: Conceptualization (Equal), Data curation (Equal), Formal analysis (Equal), Software (Equal), Supervision (Equal).

REFERENCES

- Abbas Q, Ilyas S, Saleem M, Alvi F, Din RU, Shahzad M, Sultana I and Razaq A. Fabrication and Characterization of Metal Oxide and Lignocelluloses Fibers based Working Electrode for Dye-Sensitized Solar Cells (DSSCs). *Materials Research Express* 2020; 6(12) : 1-15.
- Aba-Guevara, Cinthia G, Medina-Ramírez, Iliana E, Hernández-Ramírez, Aracely, Jáuregui-Rincón, Juan, Antonio LAJ and Luis RLJ. Comparison of two synthesis methods on the preparation of Fe, N-Co-doped TiO₂ materials for degradation of pharmaceutical compounds under visible Light. *Ceramics International* 2017; 43(6):5068-5079.
- Al-Attafi K, Nattestad A, Yamauchi Y, Dou SX, and Kim JH. Aggregated mesoporous nanoparticles for high surface area light scattering layer TiO₂ photoanodes in Dye-sensitized Solar Cells. *SCIENTIFIC REPORTS* 2017; 7(1):10341.
- Barbé CJ, Arendse F, Comte P, Jirousek M, Lenzmann F, Shklover V and Grätzel M. Nanocrystalline Titanium Oxide Electrodes for Photovoltaic Applications 1997; 80(12): 3157 – 3171.
- Bezira NÇ, Evcinb A, Kayalic R, Özenc MK and Balyaci G. Comparison of Pure and Doped TiO₂ Thin Films Prepared by Sol-Gel Spin-Coating Method. *ACTA PHYSICA POLONICA A* 2017; 132(3):620-624.
- Baglio V, Girolamo M, Antonucci V, Aricò AS. Influence of TiO₂ Film Thickness on the Electrochemical Behaviour of Dye-Sensitized Solar Cells. *International Journal of electrochemical science* 2011; 6: 3375 – 3384.
- Colmenares JC, Varma RS and Lisowski P. Sustainable hybrid photocatalysts: titania immobilized on carbon materials derived from renewable and biodegradable resources. *Green Chem* 2016; 18 : 5736-5750
- Chilev C, Stoycheva Y, Dicko M, Lamari F, Langlois P, Pentchev I. A new procedure for porous material characterization. *International Journal of Science, Technology and Society* 2017; 5(4):131 – 140.
- Donar YO, Bilge S and Sinag A. Utilisation of lignin as a model biomass component for preparing a highly active photocatalyst under UV and visible light. *Materials Science in Semiconductor Processing* 2020; 118(1):105151.
- Dhonde M, Sahu K, Murty VVS, Nemala SS, Bhargava P and Mallick S. Enhanced photovoltaic performance of a dye sensitized solar cell with Cu/N Co-doped TiO₂ nanoparticles. *Journal of Materials Science: Materials in Electronics* 2018; 29 : 6274 – 6282.
- Dhonde M, Sahu K, Murty VVS. Cu-doped TiO₂ nanoparticles/graphene composites for efficient dye-sensitized solar cells. *Solar Energy* 2020; 220 : 418 – 424.
- Etacheria V, Valentinc CD, Schneiderd J, Bahnemannd D and Pillai SC. Visible-light activation of TiO₂ photocatalysts: Advances in theory and experiments. *Journal of Photochemistry and Photobiology C: Photochemistry Reviews* 2015; 25:1–29.
- Fan K, Yu J and Ho W. Improving photoanodes to obtain highly efficient dye-sensitized solar cells:a brief review. *Materials Horizons* 2017; 4(3):319-344.

- Hagfeldt A, Boschloo G, Sun L, Kloo L and Pettersson H. Dye-Sensitized Solar Cells. *Chem.Rev* 2010; 110:6595-6663.
- Garcia-Negron V, Phillip ND, Li J, Daniel C, Wood D, Keffer DJ, Rios O and Harper DP. Processing-Structure-Property Relationships for Lignin-based Carbonaceous Materials used in Energy Storage Applications. *Energy Technology, Generation, Conversion, Storage, Distribution* 2017; 5(8):1311-1321.
- Ghann W, Kang H, Sheikh T, Yadav S, Chavez-Gil T, Nesbitt F and Uddin J. Fabrication, optimization and characterization of Natural Dye sensitized solar cell. *Scientific Reports* 2017; 7:41470.
- Gindl-Altmuttera W, Köhnke J, Unterweger C, Gierlinger N, Keckes J, Zalesak J, and Rojase OJ. Lignin-based multiwall carbon nanotubes. *Composites Part* 2019; 121 : 175 – 179.
- Gupta A , Sahuc K, Dhonde M and Murty VVS. Novel synergistic combination of Cu/S co-doped TiO₂ nanoparticles incorporated as photoanode in dye sensitized solar cell. *Solar energy* 2020; 203 : 296 – 303.
- Graetzel M, Janssen RAJ, Mitzi DB and Sargent EH. Materials interface engineering for solution – processed photovoltaics. *Nature* 2012; 488 : 304 – 312.
- Grätzel M. Dye-sensitized solar cells. *Journal of Photochemistry and Photobiology C: Photochemistry Reviews* 2003; 4:145–153.
- Grätzel M, Janssen RAJ, Mitzi DB and Sargent EH. Materials interface engineering for solution-processed photovoltaics. *NATURE* 2012; 488:304-12.
- Guo D, Zhang J, Sha L, Liu B, Zhang, Zhang X and Xue G. Preparation and characterization of lignin – TiO₂ UV – shielding composite material by induced synthesis with nanofibrillated cellulose. *BioResources* 2020; 15(4):7374 – 7389.
- Huang WY and Hsieh TL. Dyes Amount and Light Scattering Influence on the Photocurrent Enhancement of Titanium Dioxide Hierarchically Structured Photoanodes for Dye-Sensitized Solar Cells. *Coatings* 2020; 10(1),13.
- Ito S, Nazeeruddin MK, Liska P, Comte P, Charvet R, Péchy P, Jirousek M, Kay A, Zakeeruddin SM and Grätzel M. Photovoltaic Characterization of Dye-sensitized Solar Cells: Effect of Device Masking on Conversion Efficiency. *PROGRESS IN PHOTOVOLTAICS: RESEARCH AND APPLICATIONS* 2006; 14(7):589-601.
- Ibrahim MNM, Iqbal A, Shen CC, Bhawani SA and Adam F. Synthesis of lignin based composites of TiO₂ for potential application as radical scavengers in sunscreen formulation. *BMC Chemistry* 2019; 13:17.
- Jeng MJ, Wung YL, Chang LB and Chow L. Dye-Sensitized Solar Cells with Anatase TiO₂ Nanorods Prepared by Hydrothermal Method. *International Journal of Photoenergy* 2013; 2013:280253.
- Jeng MJ, Wung YL, Chang LB and Chow L. Particle Size Effects of TiO₂ Layers on the Solar Efficiency of Dye-Sensitized Solar Cells. *International Journal of Photoenergy* 2013; 2013:563897.
- Leonowicz A, Matuszewska A, Luterek J, Ziegenhagen D, Wojtás-Wasilewska M, Cho NS, Hofrichter M and Rogalski J. Biodegradation of lignin by white rot fungi. *Fungal Genetics and biology* 1999; 27(2-3):175-185.
- Lee CH, Rhee SW and Choi HW. Preparation of TiO₂ nanotube/nanoparticle composite particles and their applications in dye-sensitized solar cells. *Nanoscale Research Letters* 2012; 7:48.
- Lu Y, Lu YC, Hu HQ, Xie FJ, Wei XY and Fan X. Structural Characterization of Lignin and Its Degradation Products with Spectroscopic Methods. *Hindawi Journal of Spectroscopy*, 2017; 2017 : 8951658.
- Mathew S, Yella† A, Gao P, Humphry-Baker R, Curchod BFE, Ashari-Astani N, Tavernelli I, Rothlisberger U, Nazeeruddin MK and Grätzel M. Dye-sensitized solar cells with 13% efficiency achieved through the molecular engineering of porphyrin sensitizers. *NATURE CHEMISTRY* 2014; 6:242-247.
- Matthews D, Infelta P and Grätzel M. Calculation of the photocurrent-potential characteristic for regenerative, sensitized semiconductor electrodes. *Solar Energy Materials and Solar Cells* 1996; 44(2):119-155.
- Mohamad AA. Absorbency and conductivity of quasi-solid-state polymer electrolytes for dye-sensitized solar cells: A characterization review. *Journal of Power Sources* 2016; 329:57-71.
- Müller AV, Wierzbna WM, Pastorellia MN and Polo AS. Interfacial Electron Transfer in Dye-Sensitized TiO₂ Devices for Solar Energy Conversion Energy Conversion. *J. Braz. Chem. Soc* 2021; 32(9):1711-1738.
- Nunes VF, Lima FM, Teixeira ES, Júnior PHFM, Almeida AFL, Freire FNA. Effects of tin on the performance of ZnO photoanode for DSSC. *REVISTA MATÉRIA* 2021, 26(4):articles e13112.
- Ni M, Leung MKH, Leung DY, Sumathy K. An analytical study of the porosity effect on dye-sensitized solar cell performance. *Solar Energy Materials & Solar Cells* 2006; 90(9):1331–1344.
- O'Regan B, Grätzel M. A low-cost, high-efficiency solar cell based on dye-sensitized colloidal TiO₂ films. *Nature* 1991; 353:737-740.
- Pan K, Zhou W, ian G, Pan Q, Tian C, Xie T, Dong Y, Wang D and Fu H. Dye – sensitized solar cells based on large-pore mesoporous TiO₂ with controllable pore diameters. *Berichte der deutschen chemischen Gesellschaft* 2011; 30(30):4730.
- Kakiage K, Aoyama Y, Yano T, Oya K, Fujisawab JI and Hanaya M. Highly-efficient dye-sensitized solar cells with collaborative sensitization by silyl-anchor and carboxy-anchor dyes†. *J. Name* 2015; 51:15894-15897.
- Khan A, Nair V, Colmenares JC and Gläser R. Lignin-Based Composite Materials for Photocatalysis and Photovoltaics. *Top Curr Chem (Z)* 2018; 376(20):376:20.
- Klapiszewski L, Siwinska-Stefanska K and Kołodyn. Preparation and characterization of novel TiO₂/lignin and TiO₂-SiO₂/ lignin hybrids and their use as functional biosorbents for Pb(II). *Chemical Engineering Journal* 2017; 314:169–181.
- Kumari JMKW, Sanjeevadarshini N, Dissanayake MAK, Senadeera GKR and Thotawatthage CA. The effect of TiO₂ photoanode film thickness on photovoltaic properties of dye-sensitized solar cells. *Ceylon Journal of Science* 2016; 45(1):33-41.
- Saleem M, Irfan M, Tabassum S, Albaqami MD, Javed MS, Hussain S, Pervaiz M, Ahmad I, Ahmad A and Zuber M. Experimental and theoretical study of highly porous lignocellulose assisted metal oxide photoelectrodes for dye-sensitized solar cells. *Arabian Journal of Chemistry* 2021; 14(2):102937.

Souza APS, Oliveira FGS, Nunes VF, Lima FM, Almeida AFL, Carvalho IMMD, Manuel Graça PF. High performance SnO₂ pure photoelectrode in dye-sensitized solar cells achieved via electrophoretic technique. *Solar Energy* 2020; 211:312-323.

Shahrul AM, Abdullah MH, Mamat MH, Adilah MYS, Samat AAA, Hamzah IH, Yusnita MA and Soh ZHC. Synergistic role of aluminium sulphate flocculation agent as bi-functional dye additive for Dye – Sensitized Solar Cell (DSSC). *Optik – International Journal for Light and Electron optics* 2022; 168945.

Teixeira ES, Cavalcanti RC, Nunes VF, Júnior PHFM, Lima FM, Pinho DC, Filho MDSMDS, Almeida AFL, Freire FNA. Building and Testing a Spin Coater for the Deposition of Thin Films on DSSCs. *Materials Research*. 2020; 23(6): e20200214

Wang X, Guo H, Lu Z, Liu X, Luo X, Li S, Liu S, Jian L, Wu JL and Che Z. Lignin Nanoparticles: Promising Sustainable Building Blocks of Photoluminescent and Haze Films for Improving Efficiency of Solar Cells. *ACS Appl. Mater. Interfaces* 2021; 13(28):33536 – 33545.